Table V. Major M_J Components Calculated for the First Three Crystal-Field Levels of the $^4I_{15/2}$ (Ground) Multiplet[a]

level no.	major M_J components of eigenvectors[b]
1	$\pm^3/_2$ (30%), $\pm^5/_2$ (28%), $\pm^1/_2$ (12%), $\pm^{11}/_2$ (10%), $\pm^{13}/_2$ (10%), $\pm^7/_2$ (6%), $\pm^9/_2$ (4%)
2	$\pm^7/_2$ (18%), $\pm^1/_2$ (17%), $\pm^{11}/_2$ (16%), $\pm^{13}/_2$ (15%), $\pm^5/_2$ (13%), $\pm^9/_2$ (8%), $\pm^{15}/_2$ (7%), $\pm^3/_2$ (6%)
3	$\pm^{13}/_2$ (22%), $\pm^{11}/_2$ (18%), $\pm^1/_2$ (18%), $\pm^7/_2$ (13%), $\pm^9/_2$ (9%), $\pm^{15}/_2$ (8%), $\pm^3/_2$ (7%), $\pm^5/_2$ (5%)

[a] Calculations based on the Hamiltonian parameters given in Table IV for C_2 symmetry. [b] Identified according to percent (%) contributions to the complete eigenvectors.

shown in Table IV yield a baricenter fit with a root-mean-square deviation of 5.1 cm^{-1}. These atomic parameters were used in both our *final* C_4 and *final* C_2 crystal-field calculations. The crystal-field calculations were started out at many different points in the B_{km} parameter space, and they generally converged reasonably rapidly to yield the B_{km} values listed in Table IV. However, our empirical data set of 54 levels is not sufficient to support a truly definitive C_2 analysis.

Discussion

The polarized optical absorption measurements and energy-level analyses performed in this study clearly demonstrate that the 4f-electron/crystal-field interactions in $Er(C_2O_4)(C_2O_4H)\cdot 3H_2O$ do not have the tetragonal symmetry of the macroscopic crystal structure. This may be attributed to local structural distortions and electronic perturbations caused by the bioxalate hydrogen atoms, which are disordered in the macroscopic crystal structure. The presence of these hydrogen atoms in the coordination spheres of the erbium ions requires that the *actual* Er^{3+} site symmetry be no higher than C_2. Our results indicate that the crystal-field energy-level structure of Er^{3+} in $Er(C_2O_4)(C_2O_4H)\cdot 3H_2O$ can be reasonably well accounted for by a crystal-field Hamiltonian of C_2 symmetry, but they do not rule out the possible importance of lower symmetry contributions to the crystal-field interactions. The results also show that the crystal-field states within multiplets of low J values ($J = {}^3/_2$ or ${}^5/_2$) retain strong C_4^* symmetry character, whereas this is not the case for the majority of states derived from multiplets with $J > {}^5/_2$. According to our crystal-field energy-level calculations, the *ground* crystal-field level of $^4I_{15/2}$ has approximately 78% E'' (C_4^* parentage) character. Eigenvectors calculated for levels 32 ($^4S_{3/2}$) and 47 ($^4F_{3/2}$) exhibit greater than 96% E'' ($M_J = \pm^3/_2$) character, and eigenvectors calculated for levels 33 ($^4S_{3/2}$) and 48 ($^4F_{3/2}$) exhibit greater than 96% E' ($M_J = \pm^1/_2$) character. The $^4I_{15/2} \rightarrow {}^4S_{3/2}$ and $^4I_{15/2} \rightarrow {}^4F_{3/2}$ transition polarization results shown in Table III reflect these eigenvector compositions.

The atomic Hamiltonian used to fit the $4f^{11}$ J-multiplet baricenter energies of Er^{3+} in $Er(C_2O_4)(C_2O_4H)\cdot 3H_2O$ has parameter values very similar to those reported for Er^{3+} in $ErCl_3\cdot 6H_2O$[9] and in $Na_3[Er(C_4H_4O_5)_3]\cdot 2NaClO_4\cdot 6H_2O$,[7] and the SL (term) compositions of the $|4f^{11}[SL]J\rangle$ state vectors are, therefore, similar to those shown in Table IV of ref 7. This present paper reports the *first* detailed optical measurements and energy-level analysis of any $Ln(C_2O_4)(C_2O_4H)\cdot 3H_2O$ system, so our crystal-field Hamiltonian and its parametrization cannot be compared with previous studies. However, we have recently carried out optical luminescence measurements on *microcrystalline* samples of $Eu(C_2O_4)(C_2O_4H)\cdot 3H_2O$ and Eu^{3+}-doped $Y(C_2O_4)(C_2O_4H)\cdot 3H_2O$,[10] and the unpolarized $^7F_J \leftarrow {}^5D_0$ emission spectra observed for these samples are entirely compatible with the crystal-field model adopted in the present study. Each $^7F_J \leftarrow {}^5D_0$ transition manifold is split into $2J + 1$ components, and the energy-level spacings within the $^7F_1$ multiplet manifold are close to those predicted by the rank-two crystal-field parameters of Table IV (C_2 symmetry). We have not yet succeeded in preparing single crystals of the europium compounds large enough for *polarized* absorption and emission measurements. The growth of good, optical-quality crystals is exceedingly slow.

Finally, we note that neither $Er(C_2O_4)(C_2O_4H)\cdot 3H_2O$ nor Er^{3+}-doped $Y(C_2O_4)(C_2O_4H)\cdot 3H_2O$ yields any detectable photoluminescence.[10] The ligands coordinated to the Er^{3+} ions are rich in high-frequency vibrational modes, and these modes provide efficient nonradiative relaxation pathways between the relatively closely spaced J-multiplet manifolds. In the erbium compounds, the largest energy gap between multiplets is *ca.* 6200 cm^{-1} (between $^4I_{15/2}$ and $^4I_{13/2}$), which is less than 2 vibrational quanta of the water molecule's stretching modes. This may be contrasted with the $^7F_6$–$^5D_0$ energy gap in the europium compounds, which is ca. 12 500 cm^{-1}.

Acknowledgment. This work was supported by the U.S. National Science Foundation (NSF Grant CHE-8820180 to F.S.R.). We also gratefully acknowledge help and advice from Dr. Michael F. Reid, and we thank Dr. Charles O'Conner (University of New Orleans) for providing the initial crystal sample used in this study.

(10) Schoene, K. A.; Metcalf, D. H.; Richardson, F. S. Unpublished results.

Contribution from the Department of Chemistry, Texas A&M University, College Station, Texas 77843

Closed-Shell Electronic Structures for Linear L_nMXML_n Dinuclear Transition-Metal Complexes

Zhenyang Lin and Michael B. Hall*

Received March 28, 1991

The unparametrized Fenske–Hall method is used to study the closed-shell electronic requirements for a large number of linear L_nMXML_n (n = 3–6) dinuclear transition-metal complexes. The linearity of the dinuclear complexes relates closely to the two 3-center π bonds in the M–X–M unit. The occupation of the corresponding π-antibonding orbitals results in a severely bent M–X–M geometry. Linear dinuclear complexes with vertex-sharing tetrahedra, L_3MXML_3, require a d^8–d^8 closed-shell configuration. For linear L_5MXML_5 complexes with a structure of vertex-sharing octahedra, a d^4–d^4 configuration will satisfy the closed-shell requirement. Complexes L_6MXML_6 with a linear vertex-sharing pentagonal-bipyramidal geometry correspond to a d^2–d^2 closed-shell configuration.

Introduction

The large number of L_nMXML_n (n = 3–6; X = main-group atom, generally group 14–16) dinuclear transition-metal complexes form a unique class of compounds in transition-metal chemistry.[1] The M–X–M bond angles are particularly interesting, because one should be able to correlate their geometry with the bonding

(1) Herrmann, W. A. *Angew. Chem., Int. Ed. Engl.* **1986**, *25*, 56.

0020-1669/91/1330-3817$02.50/0 © 1991 American Chemical Society

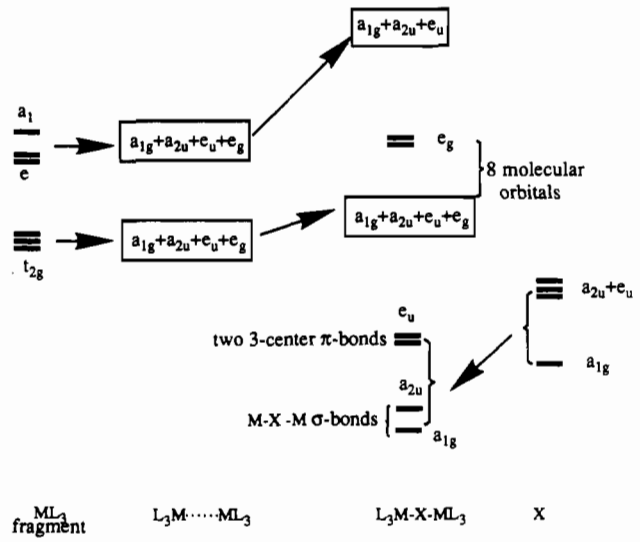

Figure 1. Orbital interaction diagram for a linear D_{3d} L_3MXML_3 complex: first column, frontier orbitals of ML_3 fragment; second column, orbitals of M_2L_6 fragment without bridging X atom; third column, orbitals of linear L_3MXML_3 complex; fourth column, valence orbitals of the bridging X atom. In the third column, the four lowest orbitals correspond to the two σ and the two π bonds in the MXM unit. The next eight orbitals are essentially nonbonding with respect to the M_2L_6 fragment.

in the M–X–M unit. A large number of linear L_nMXML_n dinuclear complexes have been synthesized and characterized structurally. In a linear M–X–M unit, the main-group atom X uses one s and one p orbital to form two σ bonds with the metals, while the other two p orbitals form corresponding π bonds. One can easily arrive at an electron count that achieves a maximum π-bonding interaction, which should insure linearity. However, there is no general theoretical approach to the relationship between their linearity and electronic closed-shell requirement although some individual molecular orbital calculations on specific complexes have been done.[2-4] In this paper, we focus on the bonding in this class of dinuclear complexes and discuss the electronic requirements for linearity.

Theory

The unparametrized Fenske–Hall molecular orbital method was used to perform the molecular orbital calculations.[5] The basis functions for all non-hydrogen atoms were generated by the numerical X_α atomic orbital program of Herman and Skillman[6a] used in conjunction with the X_α-to-Slater basis program of Bursten and Fenske.[6b] Ground-state atomic configurations were used for all non-transition-metal atoms. The transition-metal atoms assumed $d^{n+1}s^0$ cationic configurations. The exponents for the valence s and p orbitals of transition-metal atoms were determined by minimizing the energy difference between the valence eigenvalues obtained from molecular calculations and the experimental ionization potentials of $M(CO)_6$ and $M'(PF_3)_4$ (M = Cr, Mo, W; M' = Ni, Pd, Pt). The numerical X_α atomic orbitals were fit to double-ζ analytical Slater type orbitals for the valence d orbitals of transition-metal atoms and for the valence p orbitals of nontransition-metal atoms. All other orbitals were represented as single-ζ functions. The orbital exponent for hydrogen was 1.20.

L_3MXML_3 Complexes

Two diamagnetic dinuclear transition-metal complexes containing one sulfur atom linearly bridging two metal atoms, namely, $[(triphos)NiSNi(triphos)]^{2+}$ (triphos = $CH_3C(CH_2PPh_2)_3$ and $[(np_3)CoSCo(np_3)]$ ($np_3 = N(CH_2CH_2PPh_2)_3$), were reported by Sacconi and co-workers in 1975 and 1978, respectively.[7] An extended Hückel molecular orbital calculation was also reported on a model complex $[(PH_3)_3NiSNi(PH_3)_3]^{2+}$ with D_{3d} symmetry.[3] In both complexes, the metal atoms are pseudotetrahedrally coordinated by three phosphorus atoms and by one bridging sulfur atom. The metal–sulfur bond distances are unusually short (2.034 Å for Ni–S and 2.128 Å for Co–S). Because the bond angles P–M–P within MP_3 units are unusually small (between 90 and 100°), the $Co(np_3)$ and Ni(triphos) fragments correspond more closely to a ML_3 fragment derived from an octahedral complex rather than from a tetrahedral complex. Both complexes have d^8–d^8 configurations.

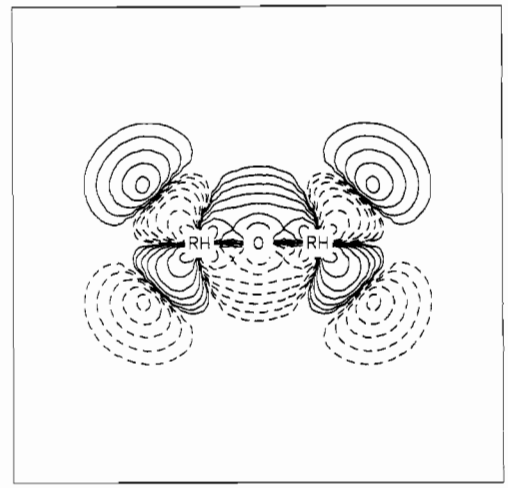

Figure 2. Contour map showing one of two 3-center π bonds (e_u bonding molecular orbitals; see Figure 1) in the Rh–O–Rh unit of the $Me_3RhORhMe_3$ complex. The plots are contoured geometrically with each contour differing by a factor of 2. The lowest contour is 0.00391 $(e/a_0^3)^{1/2}$.

Figure 1 shows a qualitative molecular orbital interaction diagram for a dinuclear L_3MXML_3 complex. It is well-known that the octahedral ML_3 fragment has three (a_1 + e) frontier orbitals and three nearly degenerate orbitals derived from the t_{2g} set. For a dinuclear bridged complex, the linear combinations between two sets of (a_1 + e) frontier orbitals transform as $a_{1g} + a_{2u} + e_g + e_u$ in D_{3d} symmetry. Since these combinations have significant s and p character, they overlap strongly with the orbitals from the bridging sulfur atom. The s and p orbitals of the bridging atom correspond to the $a_{1g} + a_{2u} + e_u$ irreducible representations of the D_{3d} point group. Therefore, the $a_{1g} + a_{2u} + e_u$ orbitals derived from the two sets of (a_1 + e) frontier orbitals interact strongly with the four atomic orbitals from the bridging atom, forming two σ bonds ($a_{1g} + a_{2u}$) and two 3-center π bonds (e_u). The e_g orbitals remain nonbonding. The linear combinations of the two t_{2g} sets transform as $a_{1g} + a_{2u} + e_g + e_u$. All except the e_g are slightly destabilized through the interaction with the bridging ligand but are essentially nonbonding orbitals. The full occupation of these eight, essentially nonbonding, orbitals corresponds to a d^8–d^8 configuration, as observed for both nickel and cobalt complexes.

A recently synthesized dinuclear rhodium complex,[8] $(C_2H_5)_6Rh_2O$, with a d^5–d^5 configuration, provides an example of partial occupation of the eight orbitals. Fenske–Hall calculation on the model complex, Me_6Rh_2O, gives an energy ordering of

$$e_g(-12.8\text{ eV}) < e_u(-11.4\text{ eV}) < a_{1g}(-10.4\text{ eV}) < a_{2u}(-9.5\text{ eV}) < e_g(-6.3\text{ eV})$$

for these eight orbitals. Thus, the rhodium complex corresponds

(2) Dunitz, J.; Orgel, L. E. *J. Chem. Soc.* **1953**, 2594.
(3) Mealli, C.; Sacconi, L. *Inorg. Chem.* **1982**, *21*, 2870.
(4) Kostic, N. M.; Fenske, R. F. *J. Organomet. Chem.* **1982**, *233*, 337.
(5) (a) Hall, M. B.; Fenske, R. F. *Inorg. Chem.* **1972**, *11*, 768. (b) Sargent, A. L.; Hall, M. B. *Polyhedron* **1990**, *9*, 1799.
(6) (a) Herman, F.; Skillman, S. *Atomic Structure Calculations*; Prentice-Hall: Englewood Cliffs, NJ, 1963. (b) Bursten, B. E.; Jensen, R. J.; Fenske, R. F. *J. Chem. Phys.* **1978**, *68*, 3320.
(7) (a) Mealli, C.; Midollini, S.; Sacconi, L. *J. Chem. Soc., Chem. Commun.* **1975**, 765. (b) Mealli, C.; Midollini, S.; Sacconi, L. *Inorg. Chem.* **1978**, *17*, 632.
(8) Hay-Motherwell, R. S.; Wilkinson, G.; Hussain-Bates, B.; Hursthouse, M. B. *Polyhedron* **1990**, *9*, 2071.

Table I. Examples of $L_{10}M_2X$ (I.e. L_5MXML_5) Dinuclear Transition-Metal Complexes[a]

complexes	M–X, Å	M–X–M, deg	d^n–d^n confign	ref
$Cp_2(CO)_4Mn_2Te$	2.459	123.80	d^5–d^5	1
$[Cl_{10}Ru_2O]^{4-}$	1.800	180.00	d^4–d^4	10
$[Cl_{10}Os_2O]^{4-}$	1.778	180.00	d^4–d^4	11
$[Cl_8(H_2O)_2Ru_2N]^{3-}$	1.720	180.00	d^4–d^4	12
$\{HB(Pz)_3\}_2(CO)_4Mo_2S$	2.200	180.00	d^4–d^4	13
$\{HB(Pz)_3\}_2(CO)_4Mo_2Se$	2.323	180.00	d^4–d^4	13
$\{HB(Me_2Pz)_3\}_2(CO)_4Mo_2S$	2.181	171.50	d^4–d^4	13
$(dppe)_2(CO)_6V_2S$	2.172	180.00	d^4–d^4	1
$Cp_2(CO)_4Mn_2Ge$	2.182	179.00	d^4–d^4	1
$Cp_2(CO)_4Mn_2Pb$	2.459	177.20	d^4–d^4	1
$Cp_2(CO)_4Cr_2S$	2.104	174.70	d^4–d^4	1
$Cp_2(CO)_4Cr_2Se$	2.200	180.00	d^4–d^4	1
$[(MeCN)_{10}Mo_2O]^{4+}$	1.847	180.00	d^3–d^3	14
$[(NH_3)_{10}Cr_2O]^{4+}$	1.821	180.00	d^3–d^3	15
$[Cl_{10}Re_2O]^{4-}$	1.860	180.00	d^3–d^3	16
$[Cl_{10}Re_2O]^{3-}$	1.832	180.00	$d^{2.5}$–$d^{2.5}$	17
$[Cl_{10}W_2O]^{4-}$	1.871	180.00	d^2–d^2	18
$[Br_{10}Ta_2N]^{3-}$	1.859	180.00	d^0–d^0	1
$[Cl_{10}Ta_2O]^{2-}$	1.880	180.00	d^0–d^0	19

[a] $HB(Pz)_3$ = hydrotris(pyrazolyl)borate, $HB(Me_2Pz)_3$ = hydrotris-(3,5-dimethyl-pyrazolyl)borate, dppe = 1,2-bis(diphenylphosphino)-ethane, and Cp = C_5H_5.

to a configuration of $(e_g)^4(e_u)^4(a_{1g})^2(a_{2u})^0(e_g)^0$. Again, the Rh–O–Rh geometry is linear, the Rh–O bond distance is short (1.89 Å), and the C–Rh–C bond angles are slightly larger than 90°. One of the two 3-center π bonds in the Rh–O–Rh unit is shown in Figure 2, where strong π interactions are clearly evident. When the Rh–O–Rh unit deviates from linearly geometry, one component of the two π-bond orbitals is significantly destabilized and the corresponding antibonding orbital is stabilized. The eight orbitals discussed above remain essentially unchanged.

A large number of $[L_3Fe–O–FeL_3]^{2-}$ (L: halide, thiolate) complexes with d^5–d^5 configurations have been characterized; most have a bent Fe–O–Fe geometry although a couple of linear molecules was reported.[9] The linear molecules, however, are suspected to be a result of orientation disorder of bent anions because of high thermal parameters of the bridging oxyen atom.[9b] In the bent complexes, the Fe–O–Fe angle ranges from 145 to 170°. The angles (ca. 108–109°) within the FeL_3 fragment in diiron complexes suggest that FeL_3 is derived from a tetrahedral ML_4 complex rather than from an octahedral ML_6 complex. The contracted d orbitals of Fe lead to weak metal ligand interactions and coupled with the tetrahedral geometry result in a high-spin d^5 metal center. Therefore, an antiferromagnetic coupling between two high-spin $S = {}^5/_2$ iron centers is usually taken as the explanation for the magnetic behavior for oxo-bridged diiron(III) complexes. The occupation of all d orbitals in these diiron complexes probably prevents the formation of Fe–O–Fe 3-center π bonds. Thus, a bent Fe–O–Fe geometry is favored.

L_5MXML_5 Complexes

The linear $L_5M(\mu_2\text{-}X)ML_5$ complexes have a structure of vertex-sharing octahedra, **1**; examples are listed in Table I. Since

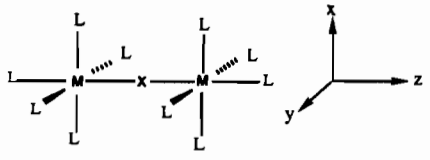

1

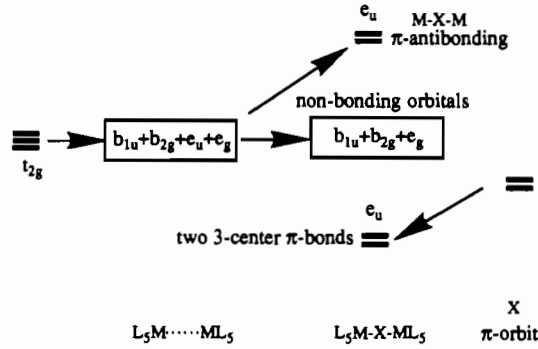

Figure 3. Orbital interaction diagram for a linear L_5MXML_5 complex: first column, t_{2g} orbitals of ML_5 fragment; second column, orbitals of M_2L_{10} fragment without bridging X atom; third column, orbitals of linear L_5MXML_5 complex; fourth column, valence orbitals of the bridging X atom. In the third column, the lowest e_u orbitals are the two π-bonding orbitals in the MXM unit and the highest e_u orbitals are the corresponding π^*-antibonding orbitals.

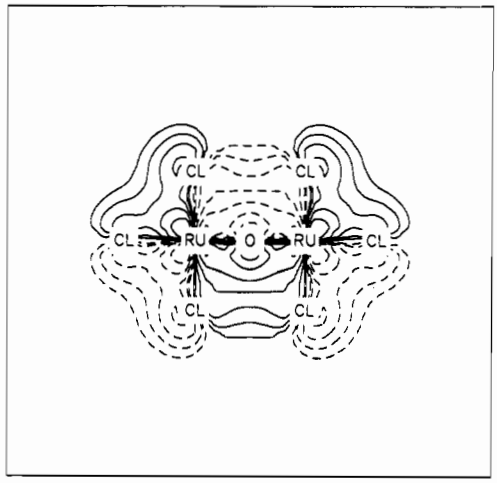

Figure 4. Contour map showing one of two 3-center π bonds (e_u bonding molecular orbitals; see Figure 3) in the Ru–O–Ru unit of the $[Cl_5RuORuCl_5]^{2-}$ complex. See Figure 2 for contour information.

the MCp fragment is isolobal with the ML_3 fragment, the Cp complexes with $CpL_2M(\mu_2\text{-}X)ML_2Cp$ formula are also included in the table. A qualitative molecular orbital picture, which has been accepted by all subsequent investigators, was first presented by Dunitz and Orgel.[2] They assumed that each metal atom contributed six atomic orbitals (i.e. sp^3d^2 hybridization) forming M–L and M–X σ bonds. Remaining on the metal atom are three d orbitals (i.e. the t_{2g} (d_{xy}, d_{xz}, d_{yz}) orbitals in the ML_6 complex), which are available for π bonding in the M–X–M unit. The linear combinations of the two t_{2g} sets transform as $e_u + e_g + b_{1u} + b_{2g}$ irreducible representations. The e_u and e_g representations correspond to the π and π^* with respect to the M···M overlap, which is, of course, vanishingly small. The strong interactions between the e_u and the bridging X atom's $p\pi$ (p_x and p_y) orbitals give rise to one set of e_u[b] bonding orbitals (i.e. two 3-center π bonds in the

(9) (a) Kurtz, D. M., Jr. *Chem. Rev.* **1990**, *90*, 585. (b) Dehnicke, V. K.; Prinz, H.; Massa, W.; Pelbler, J.; Schmidt, R. *Z. Anorg. Allg. Chem.* **1983**, *499*, 20.

(10) Deloume, J. P.; Faure, R.; Thomas-David, G. *Acta Crystallogr.* **1979**, *B35*, 558.
(11) Tebbe, V. K.-K.; Schnering, H. G. v. *Z. Anorg. Allg. Chem.* **1973**, *396*, 66.
(12) Gee, R. J. D.; Powell, H. M. *J. Chem. Soc. A* **1971**, 1795.
(13) Lincoln, S.; Soong, S.-L.; Kock, S. A.; Sato, M.; Enemark, J. H. *Inorg. Chem.* **1985**, *24*, 1355.
(14) McGilligan, B. S.; Wright, T. C.; Wilkinson, G.; Motevalli, M.; Hursthouse, M. B. *J. Chem. Soc., Dalton Trans.* **1988**, 1737.
(15) Yevitz, M.; Stanko, J. A. *J. Am. Chem. Soc.* **1971**, *93*, 1512.
(16) Morrow, J. C. *Acta Crystallogr.* **1962**, *15*, 851.
(17) Lis, T.; Jezowski-Trzebiatowski, B. *Acta Crystallogr.* **1976**, *B32*, 867.
(18) Glowiak, T.; Sabat, M.; Jezowski-Trzebiatowski, B. *Acta Crystallogr.* **1975**, *B31*, 1783.
(19) Cotton, F. A.; Najjar, R. C. *Inorg. Chem.* **1981**, *20*, 1866.

Table II. Examples of $L_{12}M_2X$ (I.e. L_6MXML_6) Dinuclear Transition-Metal Complexes

complexes	M–X, Å	M–X–M, deg	d^n–d^n confign	ref
$Cp_2(CO)_6Cr_2Te$	2.805	117.20	d^4–d^4	1
$[(CN)_{12}Mo_2S]^{6-a}$	2.172	180.00	d^2–d^2	20
$[(CN)_{12}Mo_2S]^{6-b}$	2.173	169.50	d^2–d^2	21
$[(S_2CNEt_2)_6Mo_2S]^{+b}$	1.849	180.00	$d^{1.5}$–$d^{1.5}$	22

[a] The ligand atoms in the two pentagonal planes of the dimer are in staggered positions (*a*) and in eclipsed positions (*b*).

M–X–M unit) and another set of e_u^a antibonding orbitals. The two 3-center π bonds (e_u^b) in the linear M–X–M unit are clearly indicated from the results of molecular orbital calculations. One component of the e_u^b orbitals of the $[Cl_{10}Ru_2O]^{4-}$ complex is shown in Figure 4. The remaining available orbitals ($e_g + b_{2g} + b_{1u}$) for metal d electrons are, to a first approximation, nonbonding. A diagram illustrating these orbital interactions is shown in Figure 3.

An energy ordering of $b_{2g} < b_{1u} < e_g$ was proposed by Dunitz and Orgel. They used this simple molecular orbital picture to describe the bonding in the linear complex of $[Cl_5RuORuCl_5]^{4-}$, where the e_g, b_{2g}, and b_{1u} orbitals are fully occupied. Later, an extended Hückel calculation on $[(CO)_5CrSCr(CO)_5]^{2+}$ provided a similar orbital ordering description.[3] Therefore, in the linear L_5MXML_5 complexes, eight d electrons (i.e. a d^4–d^4 configuration) are needed for the closed-shell requirement, which corresponds to full occupations of the four ($e_g + b_{2g} + b_{1u}$) nonbonding orbitals.

The orbital energy ordering is particularly important for those complexes with partial occupation of the four nonbonding orbitals. Therefore, using the parameter-free Fenske–Hall method, we calculated the molecular orbitals of the complex $[(CO)_5CrSCr(CO)_5]^{2+}$ with π-acceptor ligands and the complex $[Cl_5RuORuCl_5]^{4-}$ with π-donor ligands. For the complex with π-acceptor ligands, the orbital energy ordering of the four nonbonding orbitals ($b_{2g} < b_{1u} < e_g$) is identical with that obtained by other molecular orbital methods. However, for the complex with π-donor ligands, we found the energy ordering $e_g < b_{2g} < b_{1u}$, where the e_g orbitals are now lower than the b_{2g} and b_{1u} orbitals. To understand this result, we depict one component (**2**) of the e_g orbitals and the b_{2g} orbital (**3**). We can see that three

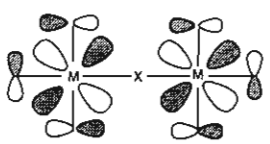

2

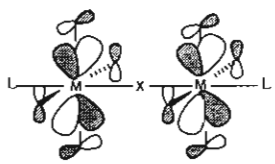

3

π-donor orbitals negatively overlap with each metal center's d orbital in the e_g orbitals, but four do so in the b_{2g} orbital. Since the b_{1u} is the out-of-phase linear combination corresponding to the in-phase b_{2g}, it too will have four antibonding interactions. Thus, for strong π donors the e_g will be more stable than the b_{2g} or b_{1u}. This ordering can be used to explain the diamagnetism of the d^3–d^3 $[Cl_{10}Re_2O]^{4-}$ complex,[16] which corresponds to a configuration of $(e_g)^4(b_{2g})^2(b_{1u})^0$.

For those complexes with intermediate ligands (e.g. NH_3 and MeCN), the exact ordering of this group of nonbonding orbitals cannot be predicted easily. The Fenske–Hall molecular orbital calculation on the $[(HCN)_{10}Mo_2O]^{4+}$ complex gives an ordering of $b_{2g} < b_{1u} < e_g$, but the $[(MeCN)_{10}Mo_2O]^{4+}$ complex is diamagnetic[14] and the actual ordering is more likely to be $e_g < b_{2g} < b_{1u}$. The error here results from an overestimation of the π-acceptor strength of AB type ligands by the Fenske–Hall method. More accurate calculations will need to be made to reproduce the experimental order in many of these intermediate cases.

For a L_5MXML_5 complex with a d^5–d^5 configuration, the antibonding orbitals e_u^a would be occupied. The occupation of these orbitals results in severe bending of the M–X–M unit. As we see from Table I, the $Cp(CO)_2MnTeMn(CO)_2Cp$ complex with a d^5–d^5 configuration has an angle of 123.8° for Mn–Te–Mn.

L_6MXML_6 Complexes

For this type of dinuclear metal complexes, the six L ligands and the bridging X atom coordinate the transition-metal atoms in a pentagonal-bipyramidal fashion. Examples are listed in Table II. Both eclipsed **4** and staggered **5** structures[21,22] are found for

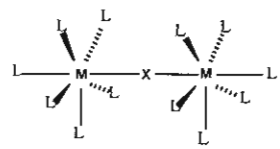

4

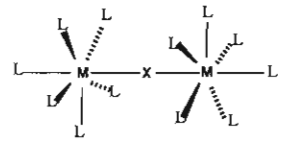

5

the $[(CN)_6MoSMo(CN)_6]^{6-}$ complex, which has a d^2–d^2 configuration. In the staggered form, the Mo–S–Mo angle is exactly 180.0°, while in the eclipsed form it is 169.5°, almost linear. The Mo–S bond distances in both complexes are similar (ca. 2.17 Å), and their value indicates strong π interactions in the Mo–S–Mo unit. The π interactions here are like those described above for the L_5MXML_5 complexes.

In a 7-coordinate pentagonal-bipyramidal complex, only two d orbitals (d_{xz}, d_{yz}) are available for d electrons. For the staggered form (D_{5d}), the linear combinations of the two (d_{xz}, d_{yz}) sets transform as e_g and e_u irreducible representations. The e_u combination interacts strongly with (p_x, p_y) orbitals of the bridging atom and yields one strongly π-bonding e_u^b (i.e. the two 3-center π bonds) and the other strongly π-antibonding e_u^a. The available e_g orbitals can accommodate four d electrons. Therefore, the d^2–d^2 configuration is the closed-shell configuration for linear L_6MXML_6 complexes. For the eclipsed form, the linear combinations of the two (d_{xz}, d_{yz}) sets transform as e_1' and e_1'' irreducible representations. The (p_x, p_y) orbitals of the bridging sulfur atom transform as e_1'. Again, a d^2–d^2 closed-shell requirement is obtained for the eclipsed form.

Since Cp is usually a tridentate ligand, we can take $Cp(CO)_3CrTeCr(CO)_3Cp$, which has a d^4–d^4 configuration, as another L_6MXML_6 complex. The severe bending in the Cr–Te–Cr unit (117.2°) and the very long Cr–Te bond distances (ca. 2.805 Å) are the result of the occupation of the M–X–M π-antibonding orbitals.

$L_4OMXMOL_4$ Complexes

Both structures **6** and **7** are found in the dinuclear transition-metal complexes with a linear M–X–M unit. Representative

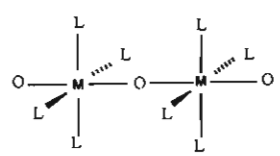

6

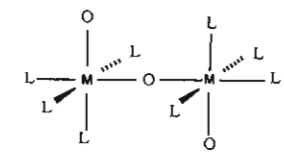

7

complexes for **6** and **7** are $Re_2O_3(S_2CNEt_2)_4$[23] and $Mo_2O_3(C_5H_4NS)_4$,[24] respectively. Surprisingly, the rhenium complex has a d^2–d^2 configuration, while the molybdenum complex has a d^1–d^1 one.

For structure **6**, we again consider the π interaction between two t_{2g} sets from the two metal atoms and three (p_x, p_y) sets from

(20) Potvin, C.; Manoli, J.-M.; Bregeault, J.-M.; Chottard, G. *Inorg. Chim. Acta* **1983**, *72*, 103.
(21) Drew, M. G. B.; Mitchell, P. C. H.; Pygall, C. F. *J. Chem. Soc., Dalton Trans.* **1979**, 1213.
(22) Broomhead, J. A.; Sterns, M.; Yang, C. G. *J. Chem. Soc., Chem. Commun.* **1981**, 1262.
(23) Fletcher, S. R.; Skapski, A. C. *J. Chem. Soc., Dalton Trans.* **1972**, 1073.
(24) Cotton, F. A.; Fanwick, P. E.; Fitch, J. W., III *Inorg. Chem.* **1978**, *17*, 3254.

the three oxygen atoms. The t_{2g} sets transform as $e_u + e_g + b_{2g} + b_{1u}$ irreducible representations. The linear combinations of the three (p_x, p_y) sets transform as $2e_u + e_g$. Because the $b_{2g} + b_{1u}$ combinations, which correspond to δ and δ^* overlaps between the two metal centers, do not correspond to any oxygen π linear combinations, they are nonbonding molecular orbitals. Thus, a d^2–d^2 configuration corresponding to the occupation of $b_{2g} + b_{1u}$ nonbonding orbitals will satisfy the closed-shell requirement for structure **6**.

Structure **7** has a C_{2h} point group. The two t_{2g} sets transform as $a_g + 2b_g + 2a_u + b_u$, while the three (p_x, p_y) sets transform as $a_g + b_g + 2a_u + 2b_u$. Since there are two b_g combinations derived from metal atoms, but only one derived from oxygen atoms, only one nonbonding metal orbital exists. This b_g orbital is depicted in **8**, where one can see that it cannot overlap with any

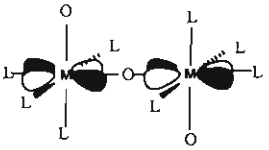

8

oxygen orbitals. Thus, only one molecular orbital is available for metal d electrons and a d^1–d^1 configuration will satisfy the closed-shell requirement.

Recently, structure **9**, which can be derived from **7** by deleting two σ ligands trans to both terminal oxygen atoms, has been found

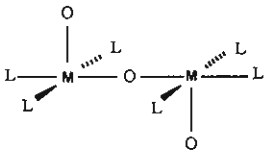

9

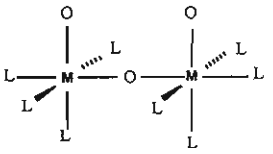

10

in two rhenium complexes,[25] $Re_2O_3Me_6$ and $Re_2O_3(CH_2SiMe_3)_6$. Both complexes have a d^1–d^1 configuration. The discussion above can be applied to structure **9**, since the missing ligands form σ bonds with metal and their loss has no effect on the π interactions. There is also cis structure, **10**, found for a molybdenum complex with d^1–d^1 configuration, e.g. $Mo_2O_3(SCNPr_2)_4$.[26] Here, the OMo–O–MoO unit is essentially planar and Mo–O–Mo is practically but not rigorously linear. It is again orbital **8**, which does not interact with any oxygen orbitals, that accommodates two d electrons.

Other Possible Geometries

The success of the bonding analysis described above has prompted us to investigate the closed-shell electronic requirements of some unknown dinuclear metal complexes and to predict the possibility of their existence. Several possible structures, **11**–**16** (Chart I), which have vertex-sharing trigonal-bipyramidal geometry, will be discussed in this section.

In a 5-coordinate trigonal-bipyramidal complex, there are four essentially nonbonding orbitals (e′ and e″ in a D_{3h} symmetry) available for d electrons. These metal orbitals are particularly important in the π bonding of the linear M–X–M unit. For structures **11** (or **12**), the eight metal orbitals (four from each metal) transform as $2e_u + 2e_g$ (or $2e' + 2e''$) irreducible representations. The strong interactions between one set of e_u (or e′) and the bridging atom's p_π (p_x, p_y) lead to a formation of two 3-center π bonds in the M–X–M unit. Thus, a full occupation of the remaining six orbitals corresponds to a d^6–d^6 closed-shell configuration. Complexes with the $(CO)_4MXM(CO)_4$ (M = Mn, Tc, Re; X = group 16 element) formula are likely to exist.

Chart I

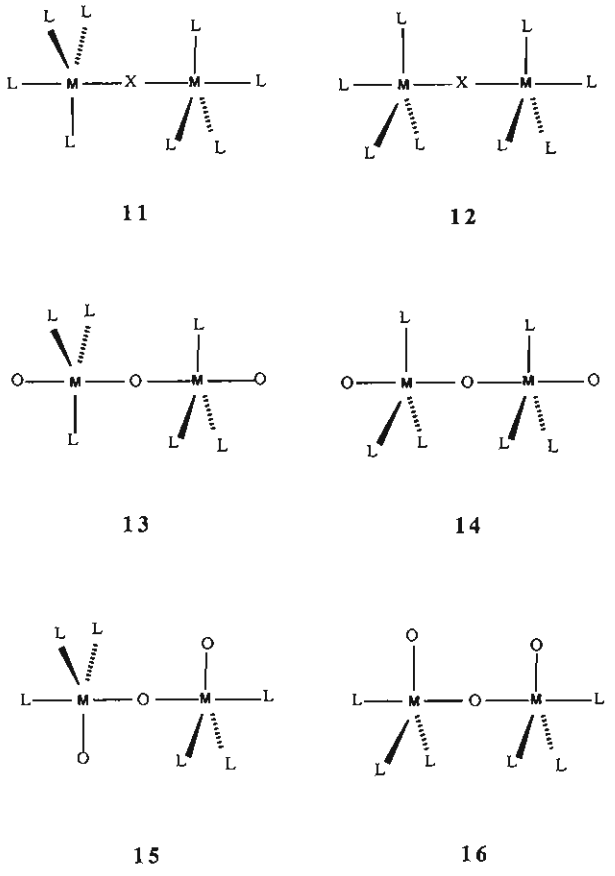

11 **12** **13** **14** **15** **16**

Table III. Closed-Shell Configurations for Linear L_nMXML_n (n = 3–6) Complexes

structure and formula	closed-shell confign
L_3MXML_3[a]	d^8–d^8
L_4MXML_4 (**11**, **12**)	d^6–d^6
OL_3MOML_3O (**13**, **14**)	d^2–d^2
OL_3MOML_3O (**15**, **16**)	d^3–d^3
OL_3MOML_3O (**9**)	d^1–d^1
L_5MXML_5 (**1**)	d^4–d^4
OL_4MOML_4O (**6**)	d^2–d^2
OL_4MOML_4O (**7**, **10**)	d^1–d^1
L_6MXML_6 (**4**, **5**)	d^2–d^2

[a] Each ML_3 fragment is derived from an octahedral complex.

For structure **13** (or **14**), the three p_π (p_x, p_y) sets derived from the three oxygen atoms transform as $2e_u + e_g$ (or $2e' + e''$). They interact strongly with the corresponding metal orbitals. Only one set of e_g (or e″) orbitals remains nonbonding. Therefore, a d^2–d^2 configuration will satisfy the closed-shell requirement. Using a similar analysis, we find that a d^3–d^3 configuration is the closed-shell requirement for structures **15** and **16**.

Summary

The discussion above indicates that the linearity of the L_nMXML_n dinuclear transition-metal complexes relates closely to the two 3-center π bonds in the M–X–M unit, since the occupation of the corresponding π-antibonding orbitals results in a severely bent M–X–M geometry. The electronic closed-shell requirements of the linear dinuclear complexes depend on the number and nature of ligands associated with the metal centers. For example, vertex-sharing tetrahedral dinuclear complexes L_3MXML_3, where each ML_3 fragment is derived from an octahedral complex, require a d^8–d^8 closed-shell configuration. For linear L_5MXML_5 complexes with a structure of vertex-sharing octahedra, a d^4–d^4 configuration will satisfy the closed-shell requirement. Complexes L_6MXML_6 with a vertex-sharing pen-

(25) Stavropoulos, P.; Edwards, P. G.; Wilkinson, G.; Motevalli, M.; Abdul Malik, K. M.; Hursthouse, M. B. *J. Chem. Soc., Dalton Trans.* **1985**, 2167.

(26) Stiefel, E. I. *Prog. Inorg. Chem.* **1977**, *22*, 1.

tagonal-bipyramidal geometry correspond to a d^2-d^2 closed-shell configuration. In Table III, we summarize the closed-shell requirements for different types of linear dinuclear transition-metal complexes. Complexes with electron counts more than the closed-shell requirements listed in Table III will have bent M-X-M structures. For complexes with electron counts less than or equal to the closed-shell requirements, linear M-X-M structures will be preferred.

Acknowledgment. We thank the National Science Foundation (Grant No. CHE 86-19420) and the Robert A. Welch Foundation (Grant No. A-648) for financial support.

Contribution from the Department of Chemistry, Purdue University, West Lafayette, Indiana 47907, and NASA Ames Research Center, Moffet Field, California 94035

Chemistry of the Scandium-Benzyne Ion in the Gas Phase

Yongqing Huang, Y. Dorothy Hill, Mariona Sodupe, Charles W. Bauschlicher, Jr., and Ben S. Freiser*

Received March 27, 1990

The gas-phase chemistry of Sc^+-benzyne with a wide variety of simple molecules is reported. The reactant ion, $ScC_6H_4^+$, was prepared from the dehydrogenation of benzene by Sc^+. $ScC_6H_4^+$ undergoes an unusual hydrogenation reaction with H_2 and D_2, as well as H/D exchange with the latter. Its reactions with a number of oxygen-containing species, XO, give ScO^+. The ability to form stable C_6H_4X neutral products from benzyne is a key factor in making this reaction exothermic. With the exception of methane, $ScC_6H_4^+$ reacts with all of the alkanes and alkenes studied to form a wide variety of product ions. A selected number of ions were subjected to more detailed structural study. Sc^+-styrene is formed from the reaction with ethane and propane. Sc^+-indane is also formed from the reaction with propane. The product ion $ScC_8H_{10}^+$ from *n*-butane is Sc^+-ethylbenzene. A prominent ion, $ScC_9H_7^+$, is formed from butadiene. Its frequent occurrence, unusual formulation, and resistance to fragmentation all indicate a high stability, with its structure most likely being that of the indenylscandium cation. $D°(Sc^+\text{-benzyne}) = 88 \pm 5$ kcal/mol was determined indirectly from the photodissociation threshold for loss of H_2 from Sc^+-benzene and from the observation that Sc^+ exothermically dehydrogenates benzene to form Sc^+-benzyne. Theoretical study indicates that the gas-phase structure is analogous to that of solid-phase mononuclear transition-metal-benzyne complexes observed crystallographically in which the metal center is coplanar with the benzyne ring and inserted symmetrically into the C-C triple bond forming a benzometallacyclopropene. The theoretical bond energy for the planar singlet $D°(Sc^+\text{-}C_6H_4) = 94$ kcal/mol is in good agreement with experiment.

Introduction

Benzyne is synthetically very useful because of its high reactivity with a wide variety of species.[1] But its high unsaturation also renders it somewhat elusive for isolation, and it has to be prepared in situ for synthetic purposes. The study of transition-metal-benzyne complexes is interesting because the highly unsaturated benzyne can be greatly stabilized by having its C-C triple bond serving as the coordinating site to the transition-metal center, thus partially compensating for the unsaturation. Some benzyne complexes have been synthesized and isolated in pure crystallized form.[2-4] Gas-phase transition-metal ions are well-known for their ability to undergo oxidative addition into the otherwise very stable C-C and C-H bonds of small hydrocarbons.[5] This, in combination with the thermodynamically driven tendency for benzyne ligand to lower its degree of unsaturation, provides an opportunity to examine the effect of the benzyne ligand on the reactivity of the metal center and vice versa. Recently we studied the chemistry of Fe^+-benzyne with a wide variety of small hydrocarbons in the gas phase.[6,7] In a typical reaction with an alkane, Fe^+ serves as a reaction initiating center via its ability to oxidatively add into C-C or C-H bonds, followed by migratory insertion of the resulting alkyl or hydrogen atom onto the benzyne ligand. Next, a β-hydrogen or alkyl is abstracted from the alkyl group and its coupling with the phenyl group and subsequent elimination of the resulting alkene ligand completes the reaction. A study of the reactions of Fe^+-benzyne with alkenes also suggests that the chemistry between them is initiated by the metal center.[7] Here we extend these studies to the reactivity of Sc^+-benzyne with some small hydrocarbons and oxygen-containing species in the gas phase, with the emphasis on determining reaction pathways and mechanisms.

Experimental Section

All experiments were performed on a prototype Nicolet FTMS-1000 Fourier transform mass spectrometer equipped with a 5.2-cm cubic trapping cell situated between the poles of a Varian 15-in. electromagnet maintained at 0.85 T.[8] The cell utilizes two stainless steel screens of 80% transmittance as the transmitter plates, permitting irradiation of the interior with a wide variety of light sources. Sc^+ was generated by focusing the beam of a Quanta Ray Nd:YAG laser (operated at 1.064 μm) onto a thin high-purity scandium target. Details of the laser desorption experiment are described elsewhere.[9]

All chemicals were obtained in high purity from commercial sources and used as supplied except for multiple freeze-pump-thaw cycles to remove noncondensable gases. Sample pressures were measured with an uncalibrated Bayard-Alpert ionization gauge and were typically 4×10^{-6} Torr for reagents and 4×10^{-5} Torr for argon, which was used for collision-induced dissociation (CID) and for collisional cooling of reactant ions.

The reactant ion, $ScC_6H_4^+$, was prepared from the dehydrogenation reaction of Sc^+ with benzene and isolated by swept double-resonance ejection pulses before its reaction with a wide variety of different samples.[10] $ScC_6H_4^+$ reacts further with benzene to form the condensation products $Sc(C_6H_4)(C_6H_6)_n^+$ (n = 1, 2). To avoid this interference, benzene was pulsed in through a General Valve Corp. Series 9 pulsed solenoid valve, triggered simultaneously with the laser desorption of the Sc target. In this way, benzene filled the cell to a maximum pressure of 10^{-5} Torr in about 150 ms and was pumped away in about 300 ms by a 6-in. diffusion pump.[11]

* To whom correspondence should be addressed at Purdue University.

(1) For a book on benzyne chemistry, see: Hoffmann, R. W. *Dehydrobenzene and Cycloalkynes*; Academic Press: New York, 1967.
(2) Bennett, M. A.; Hambley, T. W.; Roberts, N. K.; Robertson, G. B. *Organometallics* **1985**, *4*, 1992.
(3) McLain, S. J.; Schrock, R. R.; Sharp, P. R.; Churchill, M. R.; Youngs, W. J. *J. Am. Chem. Soc.* **1979**, *101*, 263.
(4) Gomez-Sal, M. P.; Johnson, B. F. G.; Lewis, J.; Raithby, P. R.; Wright, A. H. *J. Chem. Soc., Chem. Commun.* **1985**, 1682.
(5) For reviews on gas-phase transition-metal ion chemistry, see: Allison, J. In *Progress in Inorganic Chemistry*; Lippard, S. J., Ed.; Wiley-Interscience: New York, 1986; Vol. 34, p 628. Eller, K.; Schwarz, H. *Chem. Rev.*, in press.
(6) Huang, Y.; Freiser, B. S. *J. Am. Chem. Soc.* **1989**, *111*, 2387.
(7) Huang, Y.; Freiser, B. S. *J. Am. Chem. Soc.* **1990**, *112*, 1682.
(8) Cody, R. B.; Burnier, R. C.; Freiser, B. S. *Anal. Chem.* **1982**, *54*, 96.
(9) Burnier, R. C.; Byrd, G. D.; Freiser, B. S. *J. Am. Chem. Soc.* **1981**, *103*, 4360.
(10) Comisarow, M. B.; Grassi, V.; Parisod, G. *Chem. Phys. Lett.* **1978**, *57*, 413.

0020-1669/91/1330-3822$02.50/0 © 1991 American Chemical Society